



## Entrapment of collagen on polylactic acid 3D scaffold surface as a potential artificial bone replacement

Mohd Syahir Anwar Hamzah<sup>a</sup>, Celine Ng<sup>a</sup>, Nur Ismalis Shafeqa Zulkarnain<sup>a</sup>, Huda A. Majid<sup>a</sup>, Saiful Izwan Abd Razak<sup>b</sup>, Nadirul Hasraf Mat Nayan<sup>c,\*</sup>

<sup>a</sup> Faculty of Engineering Technology, Universiti Tun Hussein Onn Malaysia, KM1 Jalan Panchor, Pagoh Higher Education Hub, 84600 Pagoh, Johor, Malaysia

<sup>b</sup> Centre of Advanced Composite, Faculty of Engineering, Universiti Teknologi Malaysia, 81310 Johor Bahru, Johor, Malaysia

<sup>c</sup> Microelectronic and Nanotechnology – Shamsuddin Research Centre, Universiti Tun Hussein Onn Malaysia, 86400 Parit Raja, Johor, Malaysia

### ARTICLE INFO

#### Article history:

Received 14 June 2020

Received in revised form 25 June 2020

Accepted 12 July 2020

Available online 14 August 2020

#### Keywords:

3D Printing

Bone tissue replacement

Polylactic acid

Collagen

Hydroxyapatite

### ABSTRACT

A new potential biomimetic polymeric 3D scaffold is fabricated using collagen entrapment and 3D printed polylactic acid scaffold. The modified scaffold was characterized by compressive modulus, degree of swelling, water contact angle (WCA), and Fourier Transform Infrared Spectroscopy (FTIR). The findings show that sample PLA/col40 with 40 s entrapment duration is the optimum composition that meets the requirement for artificial bone tissue replacement. In vitro biomineralization using simulated body fluid (SBF) demonstrates that the PLA/collagen 3D scaffold is able to promote the growth of hydroxyapatite (HA) after 7 days which will subsequently improve the osteoconductive and osteoinductive properties of the 3D scaffold. The overall results suggest the potential of the 3D PLA/collagen scaffold as a prospective material for bone tissue engineering applications.

© 2020 Elsevier Ltd. All rights reserved.

Selection and peer-review under responsibility of the scientific committee of the Innovative Manufacturing, Mechatronics & Materials Forum 2020.

### 1. Introduction

Surface modification is a technique where the surface of the biomaterials is altered to realize the specified properties of materials for it to be utilized in various applications such as the medical field. Basically, surface modification is a simple method that can be implemented to attend to the majority properties of the scaffolds like mechanical strength and swelling while the surface interaction of the cells is radically changing [1,2]. However, the shortage of tissue biocompatibility and the bioactivity of synthetic materials problem remain to be resolved and improved. Thus, the biomaterials are designed to fulfil the requirement of the properties which will react or response to the cellular at molecular [3].

Poly(lactic acid) (PLA) is a biodegradable polymer that is widely used in medical application due to its excellent mechanical properties, low cost, biocompatible, and good process ability which includes 3D printing, freeze drying, solvent casting, and electrospinning [4]. Studies report that PLA is widely used in the 3D printing process as the scaffold formed possesses controllable pore size and mechanical integrity that will influence the stimulation of new

tissue formation in-vivo [5]. However, PLA does have several drawbacks due to its hydrophobic properties and lack of bioactive side-chain which result in low cell affinity and proliferation without the aid of other bioactive fillers [6]. Therefore, several strategies have been studied to improve the surface group function and reduce the hydrophobicity of PLA including covalent bonding, physisorption, or creating surface interpenetrating network by modification. In addition, there are several bioactive materials that can be used as a coating substance such as polydopamine, chitosan, collagen, gelatin, and pectin [2,4,7].

Collagen has received great attention since it possesses natural binding sites for fibroblasts and osteoblasts which are suitable to promote cell anchorage. Besides, the hydrophilic nature of collagen will help to retain fluid for nutrients transportation and accelerate the tissue formation when it is combined with the growth factors and cytokines derived from the host tissue [8–10]. Several studies have reported the potential of collagen as a bioactive coating material by combining it with other inert materials such as polycaprolactone (PCL) [8], poly (1-lactic acid-co-ε-caprolactone) (PLCL) [11], polylactic acid (PLA) [7], poly (d, l-lactide-co-glycolide) (PLGA) [12,13], hyaluronic acid [14], and poly (3-hydroxybutyrate-co-4-hydroxybutyrate) [15]. Although these strategies have been successful, the majority of the researches focus on the 2D

\* Corresponding author.

E-mail address: [nadirul@uthm.edu.my](mailto:nadirul@uthm.edu.my) (N.H.M. Nayan).

structures and conventional 3D scaffolds fabrication methods which are limited in terms of pore interconnection and porosity percentage. To date, there are limited works that investigate on collagen entrapment on the surface of 3D printed PLA scaffold.

Therefore, this study utilizes the entrapment of collagen on PLA 3D printed scaffold as such scaffold is fabricated using the additive manufacturing (AM) technique. This method promotes controlled architectures and well interconnected pores with higher porosity which are the main requisites to support the growth of new tissues. The properties of the modified PLA 3D scaffold are characterized in terms of compression modulus, wettability, morphological, and in-vitro biomineralization whereas the presence of collagen functional group is determined using the Fourier Transform Infra-red Spectroscopy (FTIR).

## 2. Materials and methods

### 2.1. Preparation of PLA 3D scaffold

The PLA (Mw, NatureWorks) scaffold is produced using an additive manufacturing technique called the desktop UP Plus 2 (3D Printing Systems, Australia) [2]. 3D scaffold is designed with the dimension of 9 mm (length) × 9 mm (width) × 9 mm (height) with 1.75 mm filament diameter. The operating conditions are indicated in Table 1.

### 2.2. Preparation of PLA/Collagen 3D scaffold

For the purpose of performing the collagen surface entrapment on the PLA scaffold (as illustrated in Fig. 1) using the facile technique, the 3D PLA samples were immersed in the collagen (Argin) containing solvent. The collagen was dissolved in acetic acid (Sigma) forming 3 w/v% collagen solution followed by the addition of acetone in the collagen containing solution with the ratio of 70:30 [7]. The printed sample was later immersed in the prepared solution at different time intervals of 10, 20, 30, 40, 50, and 60 s. Then, the sample was transferred in sodium hydroxide, NaOH (Sigma) for 1 min to neutralize the acidic solution and subjected to dry vacuum for 24 h. The scaffold was designated as neat PLA, PLA/col10, PLA/col20, PLA/col30, PLA/col40, PLA/col50, and PLA/col60.

### 2.3. Compression test

Compression test is a technique to investigate the mechanical properties of scaffold at which loads the failure may occur. The samples were placed between two plates and pressure was applied on the scaffold that compressed the distance of the scaffold. The mechanical analyzer (Brookfield Engineering Laboratories, CT3, Massachusetts, USA) fitted with a 10 kg load cell and 2 mm/min speed was fixed according to ASTM 23410/D3410 M. Based on this testing, the value of strain and stress was obtained from the compression graph as well as the value of young modulus. Five replications were conducted for each sample.

### 2.4. Degree of swelling

The initial mass of the scaffold was weighted before it was immersed in phosphate buffered saline (PBS, Sigma). The weight

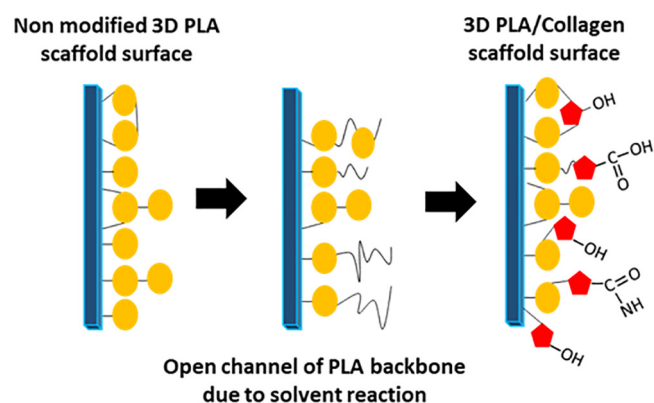


Fig. 1. Illustration of the surface entrapment process.

of the swollen scaffold was recorded after 12, 24, and 48 h and the degree of swelling was calculated using Equation (1):

$$\text{Degree of Swelling}(\%) = (w_f - w_i/w_i) \times 100 \quad (1)$$

In the equation,  $w_f$  represents the weight of the swollen scaffold at predetermined time and  $w_i$  is the initial weight of the scaffold. Five replications were conducted for each sample.

### 2.5. Water contact angle (WCA)

The WCA was measured using the sessile drop method where the image of 1  $\mu$ L of deionised water dropped on the surface of the samples was captured after 3 s using the video contact angle system (VCA Optima, Ast Products Inc). Five replications were conducted for each sample. The sample was prepared in PLA and PLA/col films by solvent casting technique using a 6 w/v% PLA in 1,4-dioxane (Sigma). Subsequently, the films were soaked into a collagen surface entrapment according to the experimental procedure aforementioned.

### 2.6. Fourier transform infrared spectroscopy (FTIR)

FTIR Spectroscopy (Perkin Elmer Frontier and Spectrum Two, Perkin Elmer) was used to determine the functional group of the PLA/Collagen scaffold within the scanning range at 400 to 4000  $\text{cm}^{-1}$  wavenumber.

### 2.7. In-Vitro biomineralization

In-vitro bioactivity of the scaffold was studied through the immersion in the simulated body fluid (SBF) solution. The SBF was prepared by dissolving reagent-grade calcium chloride ( $\text{CaCl}_2$ ), sodium chloride (NaCl), potassium chloride (KCl), magnesium chloride hexahydrate ( $\text{MgCl}_2 \cdot 6\text{H}_2\text{O}$ ), dipotassium hydrogen phosphate trihydrate ( $\text{K}_2\text{HPO}_4 \cdot 3\text{H}_2\text{O}$ ), sodium bicarbonate ( $\text{NaHCO}_3$ ), and sodium sulphate ( $\text{Na}_2\text{SO}_4$ ) in distilled water and buffered to pH 7.4 at 37 °C with tris-(hydroxymethyl)-aminomethane [ $(\text{CH}_2\text{OH})_3\text{CNH}_2$ ] and hydrochloric acid (HCl) [16] purchased from Sigma. The ionic composition and concentration of SBF are similar to the human blood plasma. The sample was immersed in 15 mL of the prepared SBF solution and placed in an incubator at 37 °C for 1 week to evaluate the growth of hydroxyapatite (HA) using the SEM microscopy.

### 2.8. Scanning electron microscope (SEM)

The SEM (Hitachi SU8010) analysis was conducted to analyze the variation of properties including the surface texture of the scaf-

**Table 1**  
Operating conditions used in the fabrication of 3D PLA scaffold.

Liquefier temperature	Printing speed	Nozzle tip size	Printing duration
200 °C	3 mm <sup>3</sup> /sec	0.20 mm	6 min

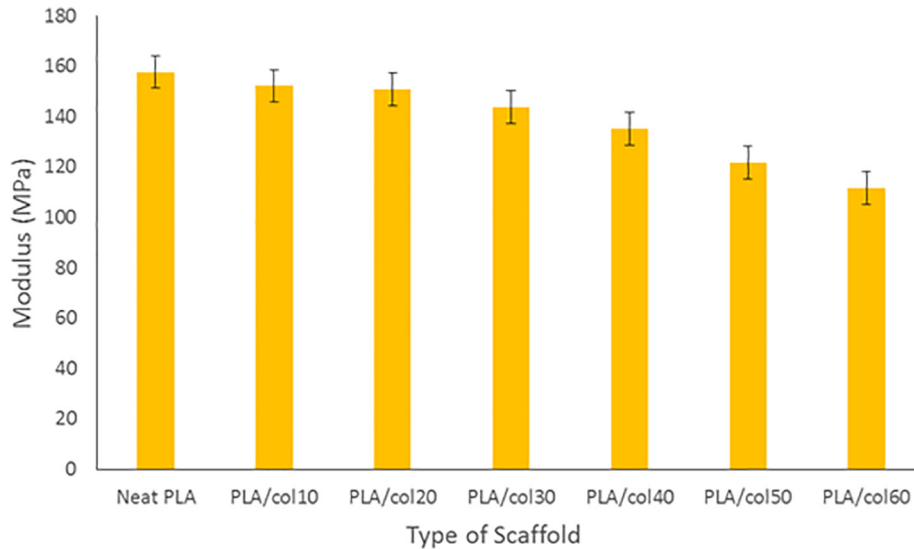


Fig. 2. Compression properties of neat PLA and PLA/col 3D scaffold.

fold. The samples of  $1\text{ cm} \times 1\text{ cm}$  were coated with gold, morphologically observed under SEM, and examined with 500 to 10000X magnification.

### 3. Results and discussion

#### 3.1. Compression test

Fig. 2 shows the compressive modulus of the neat PLA 3D scaffold and collagen modified PLA 3D scaffold. The overall trend indicates that the entrapment of collagen on the scaffold surface has lowered the compressive modulus of the neat scaffold up to 10% for 10 to 40 s exposure and up to 30% for 50 to 60 s exposure. The reduction might be due to the opening of the PLA 3D scaffold surface that leads to the loss of PLA backbone monomer when the scaffold was immersed in the solvent. Besides, collagen naturally has low mechanical properties and does not act as a reinforcement material. Hence, the main reason of including collagen is to

improve the 3D scaffold bioactivity. Therefore, the scaffold with short period is preferable where the mechanical integrity is stable as compared to longer entrapment process. Moreover, the modulus of PLA/col 3D scaffold is adequate for intervertebral disc replacement and in the range for bone tissue regeneration. Previous studies show that the typical compressive modulus of human bone is in the range of 120 to 170 MPa for femur, tibia, fibula, and humerus types, suggesting that the modified 3D scaffold is appropriate for this application [2,17]. For that reason, the PLA/collagen scaffold with the entrapment time between 10 and 40 s is suitable for future application.

#### 3.2. Hydrophilicity evaluation: Water contact angle (WCA) and degree of swelling

The hydrophilicity properties of the modified scaffold were evaluated using the degree of swelling testing and water contact angle (WCA). The swelling ratio of 3D scaffold with different

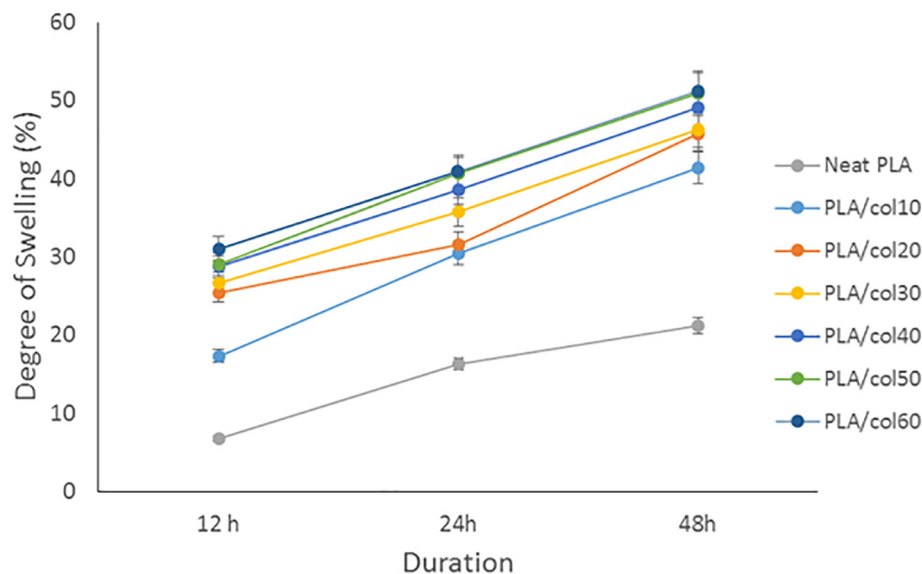


Fig. 3. Degree of swelling neat PLA and PLA/col 3D scaffold after 12, 24, and 48 h.

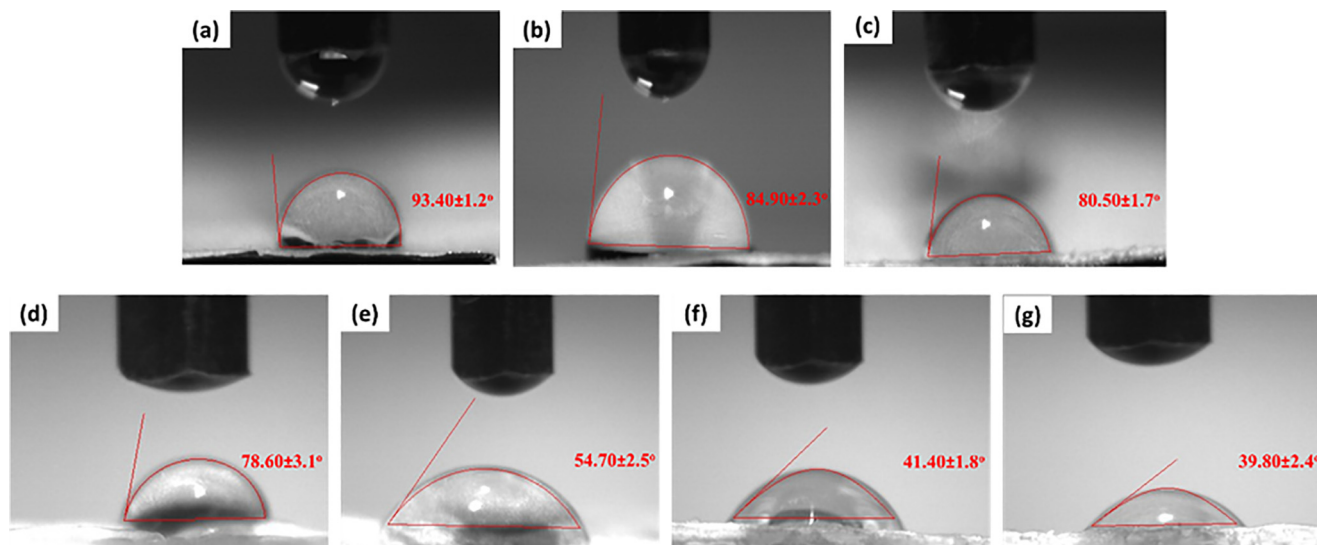


Fig. 4. WCA of (a) neat PLA, (b) PLA/coll10, (c) PLA/coll20, (d) PLA/coll30, (e) PLA/coll40, (f) PLA/coll50, and (g) PLA/coll60 3D scaffold.

soaking time in the collagen solution is presented in Fig. 3. The surface entrapment of collagen at the PLA scaffold significantly increases the swelling ratio as seen after 12 h up to four times higher than the neat 3D PLA scaffold ( $6.7 \pm 0.7\%$ ). Longer soaking time of the 3D PLA scaffold in the collagen solution decreases the hydrophobicity of the scaffold. The modified 3D scaffolds also achieve up to 50% swelling capacity after 48 h immersion as compared to the swelling percentage of neat PLA with only up to 20% from its initial weight. The presence of the collagen monomer has introduced the hydrophilic groups monomer in the PLA backbone that contain carboxyl ( $-\text{COOH}$ ), amide ( $-\text{NH}$ ), and hydroxyl ( $-\text{OH}$ ) presented in glycine, proline, as well as hydroxyproline polypeptides [10]. Besides, these functional groups act as ion exchanger reservoirs that will help to conduct certain cellular functions and play a significant role in the tissue-healing cascade [18]. The swelling percentage result of the scaffold is corroborated with the WCA as shown in Fig. 4. The contact angle of the PLA scaffold is recorded at  $93.40 \pm 1.2^\circ$  (Fig. 4a) which is higher than the modified scaffold (Fig. 4b–g) and potentially causes low cell affinity and inflammatory response towards the host tissue [7]. The surface contact angle reduction might also be contributed by the surface roughness created by the collagen bounded on the surface of the 3D PLA scaffold where it is assumed that the monomer is dispersed universally over the surface. Previous studies indicate that hydrophilic surface leads to high wettability that aids the spreading, proliferation differentiation of cells, as well as promoting the mineralization of hydroxyapatite (HA) when interacting with the human body physiological fluid environment [2]. Based on the compressive test, degree of swelling, and WCA test, the 3D PLA scaffold modified with 40 s of immersion in the collagen solution (PLA/coll40) was chosen for further analysis due to its minimal reduction in the compressive modulus and optimal hydrophilic properties.

### 3.3. Fourier transform infrared spectroscopy (FTIR)

Fig. 5a shows the characteristics peak of neat 3D PLA scaffold at  $2293.63 \text{ cm}^{-1}$  in correspond to the symmetric valence vibrations of C–H from the  $\text{CH}_3$  branch. The vibrational peak is slightly shifted to longer wavenumber for PLA/coll40 due to the  $\text{CH}_3$  branched region of collagen [4,7]. The changes from band  $1747 \text{ cm}^{-1}$  (Fig. 5a) to  $1749 \text{ cm}^{-1}$  (Fig. 5b) resulted from the  $-\text{CO}$  stretch due to the

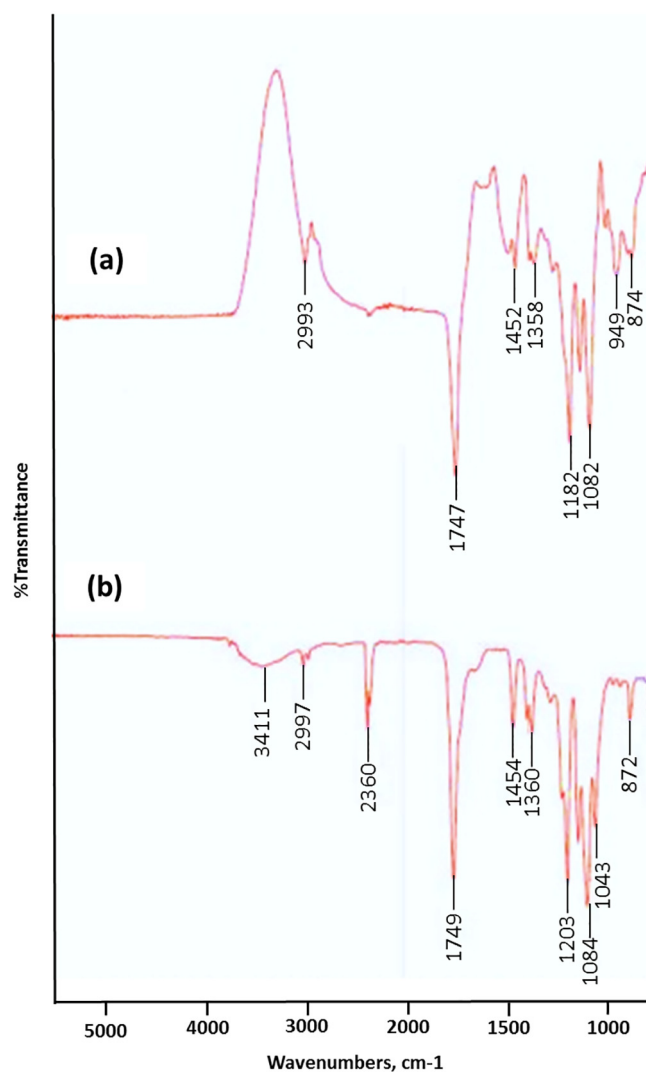


Fig. 5. FTIR spectra of (a) neat PLA (b) PLA/coll.

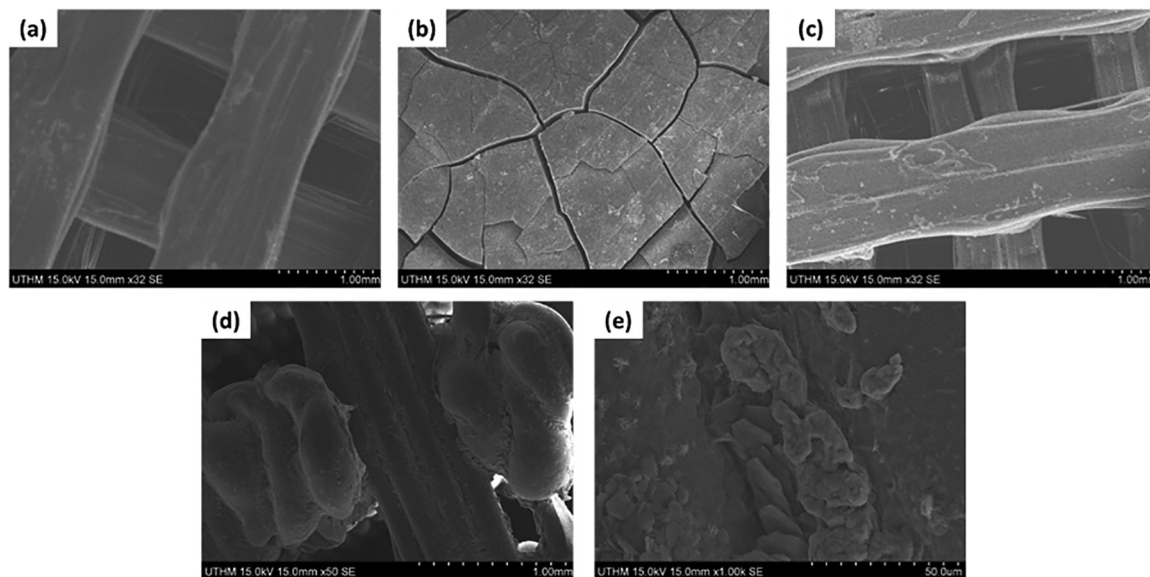


Fig. 6. SEM images of (a) neat PLA before soaked, (b) neat PLA after soaked for 7 days, (c) PLA/col40 before soaked, (d,e) PLA/col40 after soaked for 7 days.

presence of the carboxyl group ( $-\text{COOH}$ ) [19]. The spectrum between  $1000$  and  $1500\text{ cm}^{-1}$  reveals that the presence of collagen has caused the stretching vibration of the spectra values due to the presence of the carbonyl group of carboxylate ion  $\text{C}=\text{O}$  [20]. Besides, the intense peak shown in the PLA/col40 spectra at  $1454\text{ cm}^{-1}$ ,  $1360\text{ cm}^{-1}$ , and  $1182\text{ cm}^{-1}$  may contribute to the increase of the  $\text{CH}_2$ ,  $\text{CH}_3$ , and  $\text{C}-\text{N}$  monomer from the collagen towards the PLA backbone [2,4]. The new peak at  $1043\text{ cm}^{-1}$  in Fig. 5b corresponds towards the  $\text{C}-\text{O}-\text{C}$  absorptions of the carbohydrates moieties in the collagen monomer. The appearance of new peak at  $872\text{ cm}^{-1}$  for PLA/col40 is due to the overlap of the collagen monomer with the PLA backbone via the interaction of the  $\text{NH}_2$  bond of secondary amine with the PLA carbon chain. New intense peak that appeared at spectra  $2360\text{ cm}^{-1}$  represents the stretching of the  $\text{N}-\text{H}$  bond and spectra  $3411\text{ cm}^{-1}$  represents the hydroxyl group ( $\text{OH}$ ) of chitosan [19–21]. This clearly suggests that the collagen has been successfully immobilized on the 3D PLA scaffold surface.

### 3.4. In-vitro biomineralization

Fig. 6a and 6c depict the image of the neat PLA and PLA/col40 3D scaffold before it was soaked in the SBF solution. It can be seen that no major structural damage has occurred upon its modification with collagen, which is fundamental for the structural stability of bioactive coating and manipulation of scaffold [8]. During the entrapment process, the collagen was successfully immobilized onto the scaffold surface thus forming bioactive coating (Fig. 6c). Fig. 6b shows image of neat PLA after it was soaked with the SBF solution for 7 days. No hydroxyapatite (HA) was observed which indicates that the surface of the scaffold inherits low functional group for cell-recognition signal molecules. On the other hand, collagen immobilization on the 3D PLA scaffold surface was able to promote the growth of HA as shown in Fig. 6d-e. Collagen contains clustered of charged amino groups which are subjected to chelating action with calcium ions and has the ability to attract the phosphate ions and controlling formation of parallel array of oriented HA crystals. Besides, the positive net charge at the end of the collagen monomers influences the infiltration of amorphous calcium phosphate that controls the mineralization process [22–23]. This indicator initiates the potential of biomimetic PLA/col40 3D scaffold to

be used as bone graft in vivo condition for bone tissue regeneration treatment.

## 4. Conclusion

The present study demonstrates that collagen can be successfully immobilized onto 3D PLA scaffold via the surface entrapment method. The work suggests a potential procedure to overcome the limitation of poor affinity with living cells due to the lack of bioactive sites for cell adhesion and proliferation. Compressive modulus reveals that the strength reduction is adequate for bone tissue grafting replacement at the entrapment duration of up to 40 s. The collagen surface modification also improves the hydrophilic properties of the 3D PLA scaffold and subsequently promotes initial cell attachment and growth. In vitro mineralization of 3D PLA/collagen scaffold shows a huge potential to be utilized in biomimetic environs due to the rapid formation of HA as early as 7 days. In conclusion, this approach has successfully proven the 3D PLA/col40 scaffold as a new potential bone grafting material that should be further investigated on the survival of cells during in vitro culture before proceeding with the vivo transplant to reassure the effects on bone tissue regeneration.

### CRedit authorship contribution statement

**Mohd Syahir Anwar Hamzah:** Conceptualization, Investigation, Writing - original draft. **Celine Ng:** Validation, Visualization. **Nur Ismalis Shafeqa Zulkarnain:** Investigation, Formal analysis. **Huda A. Majid:** Data curation. **Saiful Izwan Abd Razak:** Methodology, Resources. **Nadirul Hasraf Mat Nayan:** Supervision, Conceptualization, Writing - review & editing.

### Declaration of Competing Interest

The authors declare that they have no known competing financial interests or personal relationships that could have appeared to influence the work reported in this paper.

### Acknowledgements

This work is supported by Universiti Tun Hussein Onn Malaysia (UTHM) through the *Geran Penyelidikan Pascasiswazah* (GPPS-Vot

number H458) as well as the Ministry of Higher Education Malaysia through the Fundamental Research Grant Scheme (FRGS-Vote number K220) and the Malaysia Technical University Network Grant Scheme (MTUN-Vote number K243 and K124).

## References

- [1] K. Shakesheff, G. Tsurpas, Surface modification to tailor the biological response, In *Tissue Engineering Using Ceramics and Polymers*, Woodhead Publishing, 2007, pp108-128.
- [2] J. Wang, N.H. Zakaria, S.I.A. Razak, M.R.A. Kadir, N.H.M. Nayan, Y. Li, K.A.M. Amin, *Compos. Interfaces* 26 (2019) 465–478.
- [3] Y.L. Cui, X. Hou, A.D. Qi, X.H. Wang, H. Wang, K.Y. Cai, Y. Ji Yin, K. De Yao, *J. Biomed. Mater. Res. A* 66 (2003) 770–778.
- [4] M.S.A. Hamzah, S.I.A. Razak, M.R.A. Kadir, S.P.M. Bohari, N.H.M. Nayan, J.S.T. Anand, *J. Polym. Eng.* 40 (2020) 421–431.
- [5] T. Lu, J. Wen, S. Qian, H. Cao, C. Ning, X. Pan, X. Jiang, X. Liu, P.K. Chu, *Biomater.* 51 (2015) 173–183.
- [6] T. Serra, M.A. Mateos-Timoneda, J.A. Planell, M. Navarro, *Organogenesis*. 9 (2013) 239–244.
- [7] M.S.A. Hamzah, A.F. Zulkifli, Z.H.A. Rais, S.I.A. Razak, N.H.M. Nayan, *J. Sustain. Sci. Manag.* 15 (2020) 20–35.
- [8] I. Sousa, A. Mendes, R.F. Pereira, P.J. Bartolo, *Mater. Lett.* 134 (2014) 263–267.
- [9] W. Jia, M. Li, L. Kang, G. Gu, Z. Guo, Z. Chen, *J. Mater. Sci.* 54 (2019) 10871–10883.
- [10] F. Lukitowati, D.J. Indrani, *Iran. J. Pham. Sci.* 14 (2018) 57–66.
- [11] W. Fu, Z. Liu, B. Feng, R. Hu, X. He, H. Wang, M. Yin, H. Huang, H. Zhang, W. Wang, *Int. J. Nanomed.* 9 (2014) 2335.
- [12] A.R. Sadeghi, S. Nokhasteh, A.M. Molavi, M. Khorsand-Ghayeni, H. Naderi-Meshkin, A. Mahdizadeh, *Mater. Sci. Eng. C* 66 (2016) 130–137.
- [13] M.V. Jose, V. Thomas, D.R. Dean, E. Nyairo, *Polym.* 50 (2009) 3778–3785.
- [14] N. Davidenko, J.J. Campbell, E.S. Thian, C.J. Watson, R.E. Cameron, *Acta Biomater.* 6 (2010) 3957–3968.
- [15] S. Vigneswari, H.P.S. Abdul Khalil, A.A. Amirul, *Int. J. Polym. Sci.* (2015).
- [16] S.I.A. Razak, I.F. Wahab, M.R.A. Kadir, A.Z.M. Khudzari, A.H.M. Yusof, F.N. Dahli, N.H.M. Nayan, T. Anand, *BioResources* 1 (2016).
- [17] A. Bandyopadhyay, S. Bernard, W. Xue, S. Bose, *J. Am. Ceram. Soc.* 89 (2006) 2675–2688.
- [18] H. Hou, B. Li, Z. Zhang, C. Xue, G. Yu, J. Wang, Y. Bao, L. Bu, J. Sun, Z. Peng, S. Su, *Food. Chem.* 135 (2012) 1432–1439.
- [19] E. Kijeńska, M.P. Prabhakaran, W. Swieszkowski, K.J. Kurzydłowski, S. Ramakrishna, *Soc. Biomater.* 100 (2012) 1093–1102.
- [20] T. Riaz, R. Zeeshan, F. Zarif, K. Ilyas, N. Muhammad, S.Z. Safi, A. Rahim, S.A. Rizvi, I.U. Rehman, *Appl. Spectrosc. Rev.* 35 (2018) 703–746.
- [21] K. Belbachir, R. Noreen, G. Gouspillou, C. Petibois, *Anal. Bioanal. Chem.* 395 (2009) 829–837.
- [22] D.A. Wahl, J.T. Czernuska, *Eur. Cells. Mater.* 11 (2006) 43–56.
- [23] F. Nudeman, K. Pieterse, A. George, P.H. Bomans, H. Friendrich, L.J. Brylka, P.A. Hilbers, G. de With, N.A. Sommerdijk, *Nat. Mater.* 9 (2010) 1004.